Supplementary Data for the Article:Site-Dependent Ambipolar Charge States Induced by Group V Atoms in a Silicon Surface

Philipp Studer, Veronika Brázdová, Steven R. Schofield, David R. Bowler, Cyrus F. Hirjibehedin and Neil J. Curson

Identified Sb and Bi features, structure and simulated DFT images

A similar set of four different features was found on the Sb and Bi doped wafer as shown in supplementary Fig. S1. The count of identified features for Sb(Bi) in sites 1-4 was 38(8), 18(4), 15(7) and 28(7) respectively. To determine the dopant reconstruction and confirm the experimental site assignment, STM topography measurements were compared to simulated STM images created from relaxed DFT cells (see supplementary methods).

STM images were simulated for Sb and Bi atoms in the original Pandey reconstructed Si(111)2×1 sites as well as for 'pushed-up' reconstructions, found to be the energetic ground states for sites 2-4. We have only observed one buckling orientation in all samples, probably due to the comparatively low doping density or carrier freeze-out at low temperatures,[32] and therefore only consider positively buckled isomers. For crystal site 1, shown in in supplementary Fig. S1a, no alternative reconstruction to the Pandey model was identified. It can be seen that the simulated STM image compares nicely to the measured STM topography image for Sb as well as Bi, reproducing the central bright feature with the two arms around it in the correct orientation. For site 2, shown in supplementary Fig. S1b, the Sb as well as the Bi atom is simply buckled upwards in the 'pushed-up' reconstruction, producing an extra bright peak in the simulated image when compared to the group V atom in the original Pandey reconstruction. This corresponds well with the experimental data, where the two adjacent up atoms and the donor are all shown as a single, bright protrusion with surrounding atoms darkened. For site 3 and 4, shown in supplementary Fig. S1c,d, substan-

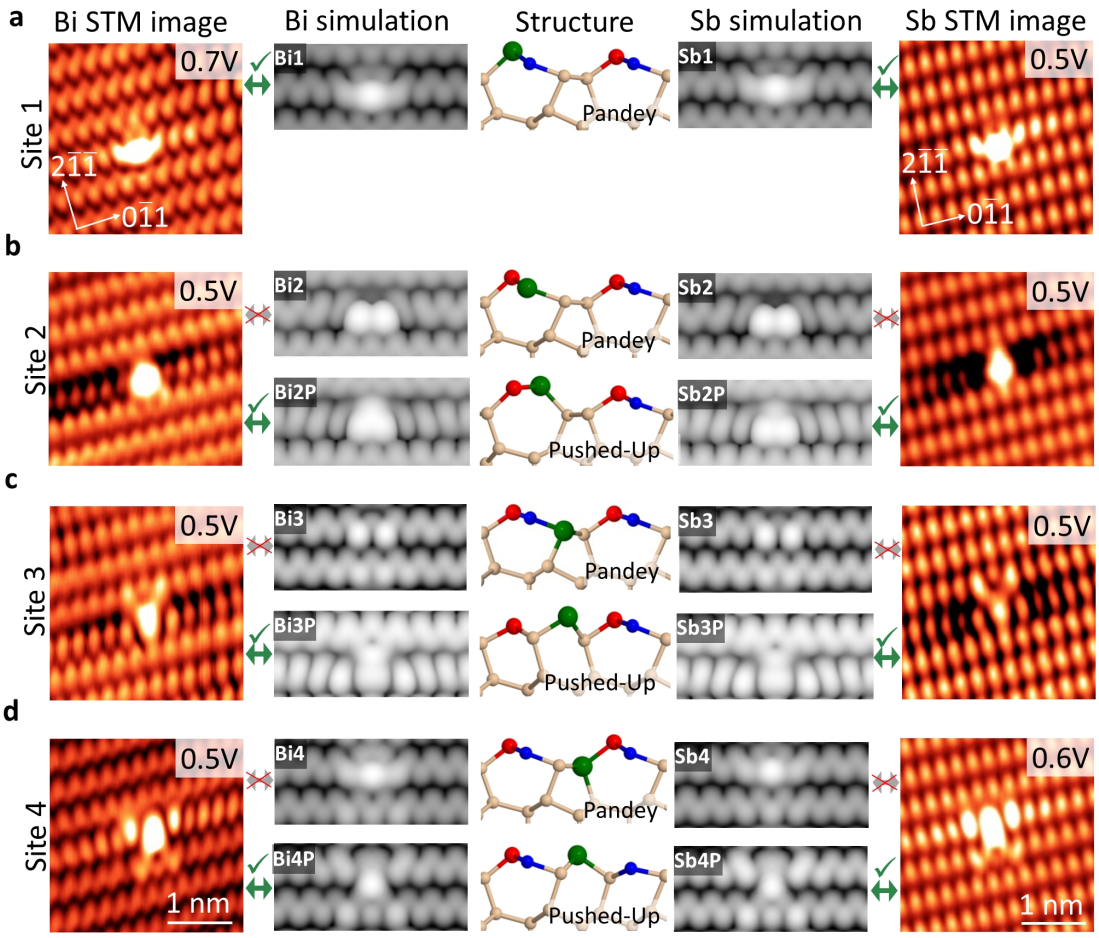

Supplementary Figure S1: (a)-(d), Bi and Sb atoms in crystal sites 1-4 respectively, comparing STM data with DFT simulations of Sb and Bi in Pandey and 'pushed-up' reconstructions. Simulated STM images are equivalent to a bias voltage of 0.5 V.

tially new reconstructions are formed in the 'pushed-up' state, leaving the dopant sticking out of the surface and being only threefold coordinated. The simulated STM images created from these atomic structure models are in excellent agreement with the observed STM contrasts, producing the bright central features with the arms and legs in the correct orientation.

The good correlation between theory and measurement confirms the experimental assignment of the observed features to the four substitutional atomic sites. Furthermore, it impressively demonstrates the fact that Sb and Bi form a new and substantially different 'pushed-up' reconstruction when incorporated into crystal sites 2, 3 and 4, as predicted by DFT ground state calculations.

Additional, not identified feature on Sb doped wafer

A fifth feature (Sb5) was found exclusively on the Sb doped wafer as shown in supplementary Fig. S2a. From the crystal symmetry of the Si(111)2×1 surface it can be experimentally determined that the feature is positioned on crystal site 1.

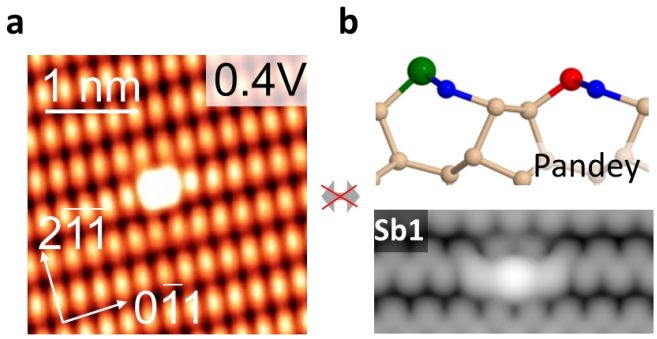

Supplementary Figure S2: (a), Additional feature identified on the Sb doped wafer, located on crystal site 1. (b), Simulated STM image, equivalent to a bias voltage of 0.5 V, showing substitutional Sb in position 1, clearly not matching the observed STM contrast.

The feature was observed 16 times, similar to the number of Sb atoms in sites 1-4. However, Sb5 did not match simulated STM images for an Sb dopant sitting substitutionally in the Pandey reconstructed site 1, as shown in supplementary Fig. S2b. A large variety of different reconstructions were explored, including locally changed buckling, missing atoms, interstitial Sb, H-adsorbates and Sb adatoms. None of the mentioned structures compared well with the observed contrast of Sb5 and its origin is therefore left unclear. Future work is needed to determine whether this feature is resulting from Sb dopants or whether it might be a general impurity present in highly doped Cz-grown wafers.

Determining charge states based on sp^3 and sp^2 hybridization

Hybridization in sp^3 or sp^2 configuration was used as an indicator to determine whether threefold coordinated surface atoms have a filled or an empty orbital respectively. π-bonded chains in the Si(111)2×1 reconstructed surface, as described by the Pandey model, are characterized by a strong buckling and an associated charge transfer from the down to the up atom.[21] The buckling allows the clean surface to reduce its energy by redistributing charge from high energy p-like orbitals

into lower energy s-like orbitals,[33] whereby the up atom forms an sp^3 hybridization and the down atom hybridizes in sp^2 configuration. This is illustrated in supplementary Fig. S3a,b.

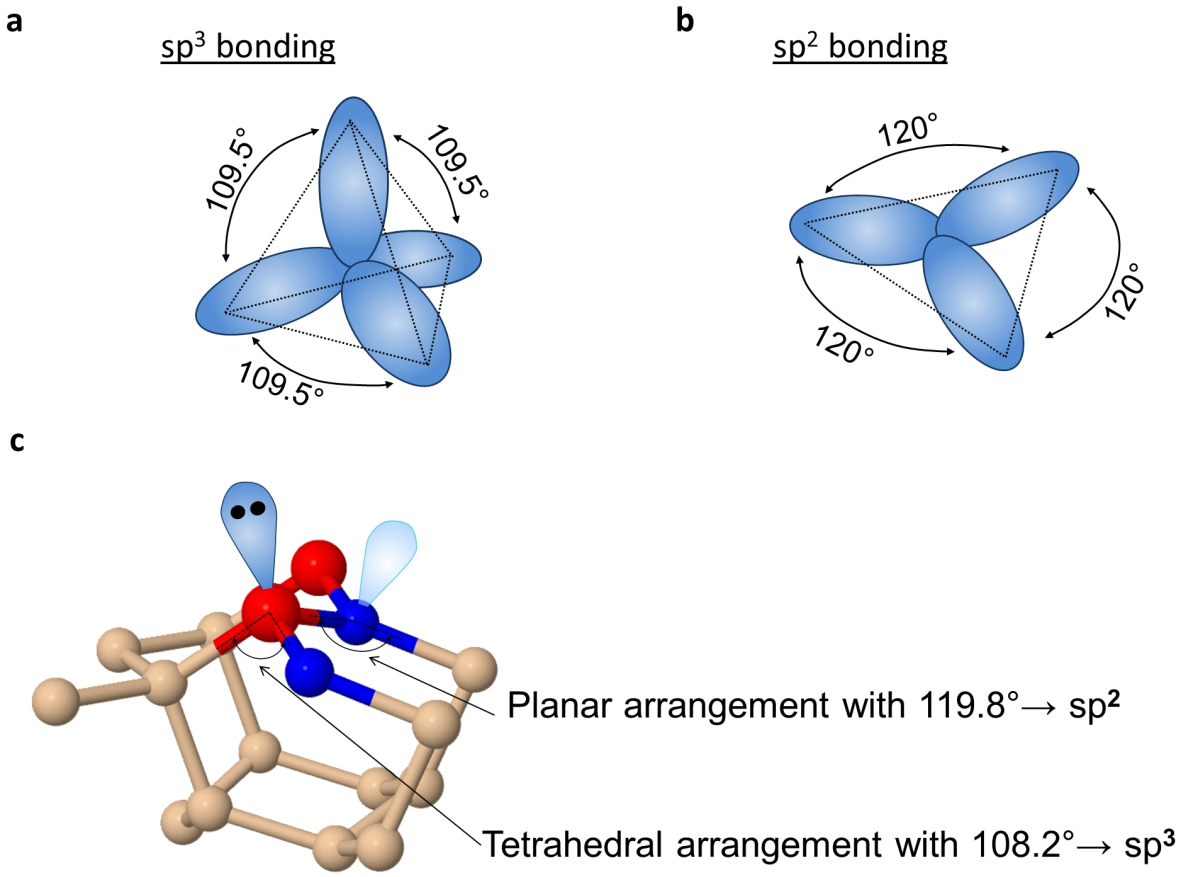

Supplementary Figure S3: (a), Orbitals hybridized in sp^3. (b), Orbitals hybridized in sp^2. (c), Bond angles extracted from DFT simulations of the Si(111)2×1 reconstructed surface.

Atoms hybridized in sp^3 are characterized by four hybridized orbitals in a tetrahedral configuration with an angle of 109.5° in between them, as shown in supplementary Fig. S3a. This corresponds well with the up atom configuration extracted from relaxed DFT cells as shown in supplementary Fig. S3c, where a tetrahedral bond configuration with an average angle of 108.2° was found between the three bonds. The fourth sp orbital is filled and points upwards, contributing to the surface valence band. Atoms hybridized in sp^2 are on the other hand characterized by three hybridized orbitals in a planar configuration with an angle of 120° in between them, as shown in supplementary Fig. S3b. This corresponds well to the down atom of the π-bonded chain, shown in supplementary Fig. S3c, where a planar configuration and an average bond angle of 119.8° was extracted from DFT simulations. The fourth, unhybridized p orbital corresponds to the empty

orbital on the down atom, sticking upwards and contributing to the surface conduction band.

In the π-bonded chains the up and down atoms therefore have a filled and an empty lone pair respectively, forming a balanced charge distribution responsible for the observed Si(111)2×1 band structure. To accurately describe the measured charge around donor atoms we must therefore not only consider their ionization state but also have to evaluate the influence of their presence onto the charge distribution within their atomic scale environment. This evaluation was done using relaxed DFT models, extracting filled and empty orbitals based on bond angles and sp^2 or sp^3 hybridization, equivalent to the clean surface discussed before. DFT can also be used to directly determine the number of electrons located in proximity to an atom and we found that results for both methods were equivalent. The extracted filled and empty orbitals allow us to determine the charge of the dopant in combination with its atomic scale environment, as shown in the main body of the paper.

Supplementary Methods

Implanting Bi for XSTM

To study individual Bi atoms at the atomic scale, we have developed a process that allows us to measure implanted Bi dopants using cross sectional STM. A similar approach was previously demonstrated by Hirayama *et al.*,[34] who implanted boron (B), cleaved the sample and subsequently annealed it *in situ*. To avoid dopant diffusion and study Bi donors in intrinsic silicon crystal sites, we however aimed to develop a process where defects are removed with an ex situ anneal before samples are cleaved. Phosphorus doped Si(211) wafers with a donor concentration of 1×10^{15} cm^{-3}, purchased from Virginia semiconductors, were used as a substrate. The low phosphorus dopant concentration was required to provide suitable conductivity for STM measurements at 78 K while simultaneously ensuring that measurements were not influenced by the phosphorus dopants, since less than one dopant is expected in the surface of a one square micrometer image. Bi was implanted into this wafer to a depth of 600 nm with a uniform concentration of 1×10^{20}

cm^{-3}, using five different implantation energies of 250 keV, 500 keV, 850 keV, 1350 keV and 2000 keV respectively. To remove implantation damage and recover the monocrystalline structure in a solid phase epitaxial regrowth process, samples were annealed in two steps to 650 C for 3 min and then to 1000 C for 3 min. Subsequent Hall measurements confirmed an active Bi dopant concentration of 7.2×10^{18} cm^{-3}. The difference in concentration between implanted and electrically active Bi is expected, as Bi is known to precipitate and diffuse towards the sample surface upon annealing.[35] The remaining active Bi concentration is nonetheless sufficient to study individual Bi atoms as it corresponds to a surface density of over 10 dopants in the area of a 100 nm square image. Remaining implantation damage was found to be suitably low to allow investigating the sample with XSTM.

Density Functional Theory Simulations

To compensate for the fact that our sample is not intrinsic silicon but heavily doped n-type silicon, we use the established practice of modifying the simulation cell by adding one electron.[15] The high dopant concentration results in a Fermi level (E_F) that is pinned at the Si(111)2×1 surface and therefore located slightly above the onset of the surface conduction band.[14] This in turn leads to an accumulation of electrons, filling states at the bottom of the surface conduction band. We found that it was necessary to shift the Fermi level slightly into the surface conduction band in order to accurately model the influence of the Fermi level pinning when simulating STM images. This is in good agreement with previously published simulations of this surface.[13] Different methods to simulate the Fermi level pinning were tested, namely a manual shift of the Fermi level when simulating STM images, the introduction of a dopant atom into the simulated semiconductor bulk of the cell and the addition of a single electron into the cell. The effect of all three different methods was found to be very similar and we therefore chose to add a single electron to all our cells, a well-established method for silicon surfaces.[15]

We used density functional theory with the gradient-corrected Perdew-Burke-Ernzenhof exchange-correlation functional,[31] as implemented in the Vienna Ab-Initio Package code.[30, 36] VASP adds a neutralizing background charge for charged systems. The core electrons were described by the

projector augmented-wave method.[37, 38] All calculations were spin-polarized. The plane-wave basis set kinetic energy cutoff was set to 250 eV. The lattice parameter of bulk Si had been optimized. The slab unit cell parameters were 30.936 Å x 13.387 Å x 30.000 Å. The Brillouin zone was sampled using a (2x3x1) Monkhorst-Pack[39] k-point mesh. Gaussian smearing was used for fractional occupancies, with a 0.1 eV width. STM images were simulated using the Tersoff-Hamann approach.[40]

Supplementary References

32. Bussetti, G. *et al.* Coexistence of Negatively and Positively Buckled Isomers on n+-Doped Si(111)-2x1. *Phys. Rev. Lett.* **106,** 067601 (2011).

33. Badziag, P. & Verwoerd, W. S. Cluster Study of the Si(111)2x1 Reconstruction. *Surf. Sci.* **201,** 87–96 (1988).

34. Hirayama, H., Koike, M., Einaga, Y., Shibata, A. & Takayanagi, K. Cross-Sectional Scanning Tunneling Microscope Study of a Boron-Implanted Si Wafer. *Phys. Rev. B* **56,** 1948 (1997).

35. Wagh, A. G., Bhattacharya, P. K. & Kansara, M. J. Furnace and Laser Annealing of Bismuth Implanted Silicon. *Nucl. Instrum. Methods* **191,** 96–100 (1981).

36. Kresse, G. & Furthmüller, J. Efficient Iterative Schemes for Ab Initio Total-Energy Calculations using a Plane-Wave Basis Set. *Phys. Rev. B* **54,** 11169–11186 (1996).

37. Blöchl, P. E. Projector Augmented-Wave Method. *Phys. Rev. B* **50,** 17953–17979 (1994).

38. Kresse, G. & Joubert, D. From Ultrasoft Pseudopotentials to the Projector Augmented-Wave Method. *Phys. Rev. B* **59,** 1758–1775 (1999).

39. Monkhorst, H. J. & Pack, J. D. Special Points for Brillouin-Zone Integrations. *Phys. Rev. B* **13,** 5188–5192 (1976).

40. Tersoff, J. & Hamann, D. R. Theory of the Scanning Tunneling Microscope. *Phys. Rev. B* **31,** 805–813 (1985).